Coarsening of Antiferromagnetic Domains in Multilayers: The Key Role of Magnetocrystalline Anisotropy

D. L. Nagy,[1] L. Bottyán,[1] B. Croonenborghs,[2] L. Deák,[1] B. Degroote,[2] J. Dekoster,[2] H. J. Lauter,[3] V. Lauter-Pasyuk,[4,5] O. Leupold,[6] M. Major,[1,2] J. Meersschaut,[2] O. Nikonov,[3,4] A. Petrenko,[4] R. Rüffer,[6] H. Spiering,[7] and E. Szilágyi[1]

[1]*KFKI Research Institute for Particle and Nuclear Physics, P.O. Box 49, H-1525 Budapest, Hungary*
[2]*K. U. Leuven, Instituut voor Kern- en Stralingsfysica, Celestijnenlaan 200 D, B-3001 Leuven, Belgium*
[3]*Institut Laue-Langevin, BP 156, F-38042 Grenoble Cedex 9, France*
[4]*Frank Laboratory of Neutron Physics, Joint Institute for Nuclear Research, 141 980 Dubna, Moscow Region, Russia*
[5]*Technische Universität München, James Franck Strasse 1, D-85747 Garching, Germany*
[6]*European Synchrotron Radiation Facility, BP 220, F-38043 Grenoble, France*
[7]*Institut für Anorganische Chemie und Analytische Chemie, Johannes Gutenberg Universität, D-55099 Mainz, Germany*

(Received 29 May 2001; published 29 March 2002)

The domain structure of an antiferromagnetic superlattice is studied. Synchrotron Mössbauer and polarized neutron reflectometric maps show micrometer-size primary domain formation as the external field decreases from saturation to remanence. A secondary domain state consisting mainly of at least 1 order of magnitude larger domains is created when a small field along the layer magnetizations induces a bulk-spin-flop transition. The domain-size distribution is reproducibly dependent on the magnetic prehistory. The condition for domain coarsening is shown to be the equilibrium of the external field energy with the anisotropy energy.

DOI: 10.1103/PhysRevLett.88.157202 PACS numbers: 75.70.Kw, 75.25.+z, 75.30.Gw

Antiferromagnetically (AF) coupled metallic multilayers [1] have received much attention due to their relevance in fundamental science and technology alike. The archetype Fe/Cr system shows oscillatory interlayer coupling [2,3] and giant magnetoresistance (GMR) [4]. Magnetic and transport behavior of coupled magnetic multilayers (MMLs) is affected by static and dynamic properties of the domain structure. Domain-size-dependent resistance noise may be as large as to limit GMR-sensor applications [5]. Nevertheless, our direct knowledge on the domain structure is limited to a few thick trilayer studies [6,7]. This is related to the difficulties in visualizing *in-plane AF domains* in a multilayer (ML) of few nm thickness. Therefore indirect methods such as resistance noise [5] and magnetoresistance [8] measurements, off-specular nonpolarized [9] and polarized neutron reflectometry (PNR) [10,11], and soft-x-ray resonant magnetic diffuse scattering [12] have been used to estimate the AF-domain-size distribution in MMLs.

In remanence, a MML is in a multidomain state. In a strongly AF-coupled ML the magnetic domain structure of the individual ferromagnetic (FM) layers is strictly correlated through the ML stack from substrate to surface. This results in zero net magnetization magnetic superstructure domains in a periodic ML of an even number of equally thick FM layers. It is in this sense the term "AF domain" is used here [13]. Kerr microscopy on AF-coupled Fe/Cr/Fe trilayers first revealed domains with "sizes" of the order of a few μm arranged in a *patchlike* pattern [6]. Let the lateral "size" of the AF domains (strictly speaking, the correlation length of the magnetization direction) be ξ. Electric transport data [5,8] on coupled polycrystalline Co/Cu sandwiches and ML samples showed $\xi \leq 1$ μm-size AF domains ["primary domain state" (PDS)] when decreasing the external field from saturation to zero. A PDS was invoked to describe the broad off-specular sheets in PNR at the AF reflection of Fe/Cr MLs in applied magnetic field [11]. The observations of the low-field behavior of the domain structure of AF MLs are, nevertheless, controversial. A *coarsening* of the domains to an average size of $\xi \geq 10$ μm ["secondary domain state" (SDS)] was observed in a small decreasing or reverting field, in other cases in small increasing external fields [5,6,8,9,14,15]. A difference in the in-plane magnetic correlation length was found by soft-x-ray resonant magnetic diffuse scattering in a Co/Cu ML when magnetized in the easy or hard direction [12]. Although the domain-wall energy is the driving force of the PDS $\rightarrow$ SDS transition, this is, in the light of the above observations, not enough to explain their diversity.

We investigated the PDS $\rightarrow$ SDS transition by off-specular synchrotron Mössbauer reflectometry (SMR) (grazing incident nuclear resonant reflection of synchrotron radiation) [16], and by PNR. For both methods, the off-specular scattering width around an AF reflection stems from the finiteness of ξ (domain structure, "magnetic roughness"). In the present Letter, using SMR and PNR, we identify the key role of magnetocrystalline anisotropy in the domain coarsening. We demonstrate that the PDS $\rightarrow$ SDS transition takes place *when the system is passing a bulk-spin-flop (BSF) transition* and that the *field history* is an important factor determining the actual domain structure.

The ML sample was grown on an MgO(001) substrate at 450 K by molecular beam epitaxy alternately

depositing ^{57}Fe from a Knudsen cell and Cr from an electron gun at a rate of 0.1 and 0.35 Å/s, respectively, and base pressure of 4×10^{-10} mbar. Using high- and low-angle x-ray diffraction as well as Rutherford backscattering an MgO(001)/[^{57}Fe(26 Å)/Cr(13 Å)]$_{20}$ *epitaxial superlattice* structure was found with MgO(001)[110] ‖ Fe(001)[100] and root mean square interface roughness of 0.4 nm. Magneto-optical Kerr effect (MOKE) and vibrating-sample magnetometry both indicated AF coupling with a saturation field $H_s \approx 0.9$ T. A schematic view of the chemical and magnetic structures of the sample is shown in the inset of Fig. 1A.

The SMR experiments were performed at the ID18 beam line of the European Synchrotron Radiation Facility, Grenoble, France [17]. The sample was placed in a superconducting split-coil magnet mounted on a goniometer.

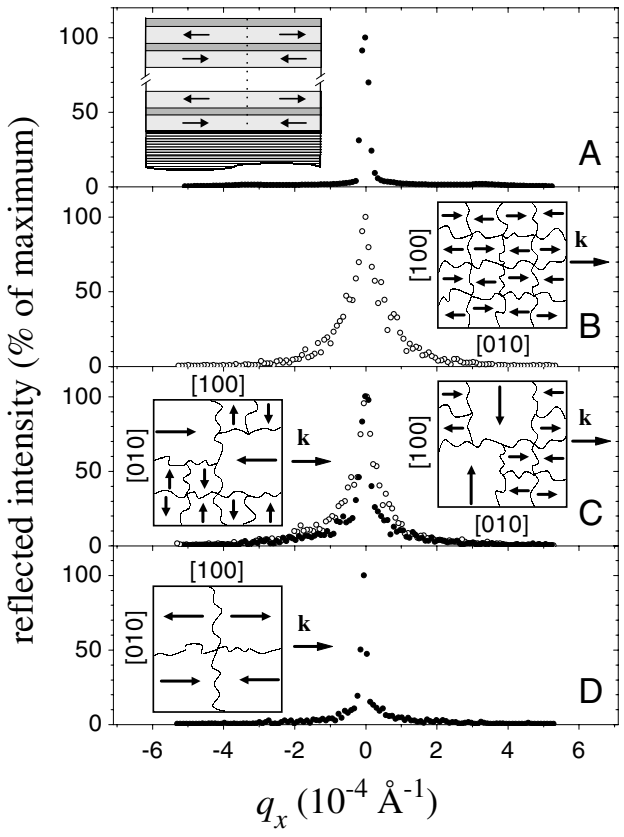

FIG. 1. Off-specular ω scans. Reflected intensity vs scattering vector component $q_x = 2k\Theta(\omega - \Theta)$ of a MgO(001)/[^{57}Fe(26 Å)/Cr(13 Å)]$_{20}$ ML at the AF Bragg-reflection ($\Theta = 0.4°$) measured in zero external magnetic field: (A) prompt reflectivity, not being dependent on magnetic field prehistory, (B)–(D) delayed reflectivity, (B) following saturation in 4.07 T, (C) following exposure to 13 mT parallel to the magnetizations (open circles: nonflipped domains; full circles: flipped domains), (D) following exposure to a field of 35 mT. The inset in (A) is a schematic side view of the chemical and magnetic structure of the sample in the vicinity of a domain wall (dotted line). The insets in (B)–(D) are schematic top views of the orientation of the crystallographic axes and of the top-layer magnetizations (short and long arrows represent small and large domains, respectively) relative to the photon wave vector **k**.

All scans were taken at (290 ± 2) K in zero magnetic field following a magnetic-field history as detailed below. The off-specular scattering was measured on the first-order AF reflection at a *fixed* angle of $2\Theta = 0.80°$ [18,19]. Photons from both the electronic (prompt) and the resonant nuclear scattering (delayed, SMR) process were recorded as a function of the angle of incidence $0 < \omega < 2\Theta$.

The PNR experiments were done at the SPN-1 polarized neutron reflectometer of Joint Institute for Nuclear Research, Dubna, Moscow, Russia [20] in in-plane static magnetic fields parallel to the linear polarization of the incoming neutrons at (286 ± 2) K. Two spin flippers were operated to change the polarization of the incoming and the scattered neutrons. The spin of the scattered neutrons was analyzed by a Soller-mirror polarizer. The neutrons reflected by the Soller mirror hit a position-sensitive detector so that the scattered neutron intensity was mapped onto the q_z-q_x plane in all (++, +−, −+, and −−) channels.

In remanence, the magnetization vectors of the Fe layers in the AF superlattice with fourfold in-plane anisotropy point parallel or antiparallel to either of the Fe[010] or Fe[100] easy axes in the film plane. Releasing the magnetic field parallel to one of the easy axes from saturation, the magnetizations settle *solely* in the perpendicular easy direction. As recently observed with PNR [21] on an equivalent and with MOKE [18] and SMR [18,19] on the same sample, an irreversible BSF transition takes place when a moderate magnetic field is applied along the easy axis in which the layer magnetizations actually lie. At a critical BSF field of $H_{SF} \approx 13$ mT, where the magnetic ("Zeeman") energy overcomes the fourfold in-plane magnetocrystalline anisotropy, the layer magnetizations jump into the perpendicular easy axis [18,19,21]. The alignment is retained in remanence. In these samples since no uniaxial anisotropy was present, the surface-spin-flop transition previously observed in Fe/Cr(211) superlattices [22,23] played no role.

In the present SMR experiment, the sample was first saturated along the Fe[100] easy direction in 4.07 T, a field well above H_S. In Fig. 1, ω scans are shown as a function of the longitudinal in-plane component $q_x = 2k\Theta(\omega - \Theta)$ of the scattering vector **q**, where $k = |\mathbf{k}|$ and **k** is the photon wave vector. When the field was released, the layer magnetizations lay in the perpendicular Fe[010] easy direction, parallel or antiparallel to **k** (inset of Fig. 1B). While a sharp specular reflection was observed in the prompt reflectivity (Fig. 1A), only a broad diffuse shoulder appeared in the SMR ω scan (Fig. 1B). On rotating the sample by 90°, the magnetizations turned perpendicular to **k**, and the AF reflections disappeared since for **k**-perpendicular hyperfine field no AF reflections are expected in $\Theta - 2\Theta$ SMR scans [16]. The intensity of the AF reflections recovered, when a field of 12 to 16 mT was applied along the Fe[010] direction perpendicular to the photon wave vector **k** and the ML passed the BSF [19]. Figure 1C shows two ω scans of

considerably different width, taken in two mutually perpendicular orientations of the sample relative to **k** following an exposure of the ML to 13 mT, halfway in the BSF transition. At this point, the flipped regions of the ML (left inset of Fig. 1C) mainly give rise to a narrow specular peak, whereas the not-yet-flipped regions (right inset of Fig. 1C) stay to show a broad diffuse shoulder in the delayed intensity. By exposing the sample to 35 mT, the BSF transition is completely passed (inset of Fig. 1D) and the ω scan is dominated by a specular peak (Fig. 1D). No further change in the shape of the ω scan could be induced by any field cycle including repeated generation of BSF transitions, until the system was fully saturated. However, exposing the sample to a 4.07 T field again, the ω scans became identical with that shown in Fig. 1B; i.e., the specular peak disappeared from the SMR ω scan.

The pure diffuse delayed reflectivity in Fig. 1B shows that the PDS is retained in zero field. The magnetic correlation length ξ of the AF domains can be calculated from the shape of the diffuse shoulders. Supposing an exponential autocorrelation function for the in-plane magnetization in the PDS, $\xi \approx 2.6\ \mu$m is estimated from the SMR peak width. The narrow specular peak following the BSF (Fig. 1D) is indicative of large domains. In this SDS, large and small flipped domains coexist, giving rise to narrow and broad components in the ω scan, respectively. Because of the finite experimental resolution in 2Θ, only a lower limit of $\xi > 16.5\ \mu$m can be deduced for the large domains. The deduced minority small flipped domain size is $\xi \approx 2.6\ \mu$m, i.e., equal to that in the PDS. Midway into the BSF transition (Fig. 1C), the nonflipped regions are in the PDS, whereas the flipped regions are in the SDS.

The domain coarsening can be monitored by polarized neutron diffuse scattering, without rotating the sample. Prior to the PNR experiment the sample was *ex situ* saturated in 2.1 T, i.e., well above H_S and mounted in zero field with magnetization parallel/antiparallel to the incident neutron polarization. PNR maps taken in increasing external field are shown in Fig. 2. Left and right columns in Fig. 2 represent non-spin-flip and spin-flip reflectivities (here R^{--} and R^{-+}), corresponding to magnetization components parallel/antiparallel and perpendicular to the neutron spin, respectively. In a field below H_{SF} (Fig. 2A) the AF reflection appears only in the non-spin-flip channels and consists of a broad diffuse sheet. In contrast, in Fig. 2C, in a field above the transition, the AF reflection is observed only in the spin-flip channels. While the non-spin-flip channels consist only of off-specular diffuse sheets, the spin-flip channels show mainly specular scattering. Midway into the transition (Fig. 2B), the AF reflection shows up in both channels, in full accordance with the SMR results.

The experiments show that the BSF transition in an antiferromagnetically coupled multilayer results in a sudden coarsening of the primary domain size by at least 1 order of magnitude. The formation of the PDS and the sudden coarsening on BSF can be understood qualitatively by the following consideration. A lateral variation of the coupling strength due to layer thickness fluctuations is unavoidable. Consequently, the saturation field H_S is also subject to a finite lateral distribution characterized by a correlation length ξ_S close to the terrace length of the ML (typically a few tens of nm). Gradually releasing the field applied along the [100] direction from full saturation, first the strongest-coupled regions have the freedom "to decide" whether their odd and even layers start rotating clockwise and counterclockwise, respectively, or vice versa [14]. Upon further decreasing the field, the layer magnetization direction of the neighboring regions becomes unstable. The minute AF domain-wall energy becomes decisive in this state and the neighboring regions nucleate on the already rotated regions, so that the sense of rotation of the individual layers is preserved. The nucleation goes on until the individual layer magnetizations settle in either the [010] or the $[0\bar{1}0]$ direction, giving rise to the observed patch structure [6] consisting of two types of domains in remanence that differ only in the order of the FM sheets (180° domain walls). Nevertheless, in the PDS $\xi > \xi_S$, since with decreasing field the domain-wall angle and, consequently, the domain-wall energy per unit area increases. Therefore, also ξ increases beyond ξ_S to decrease the domain-wall density and, thereby, to minimize the domain-wall energy. This spontaneous growth of the domains is limited by the domain-wall pinning (coercivity), and the gain in domain-wall energy is not enough to increase the average domain size beyond a certain limit. Using literature values of the Fe exchange and anisotropy

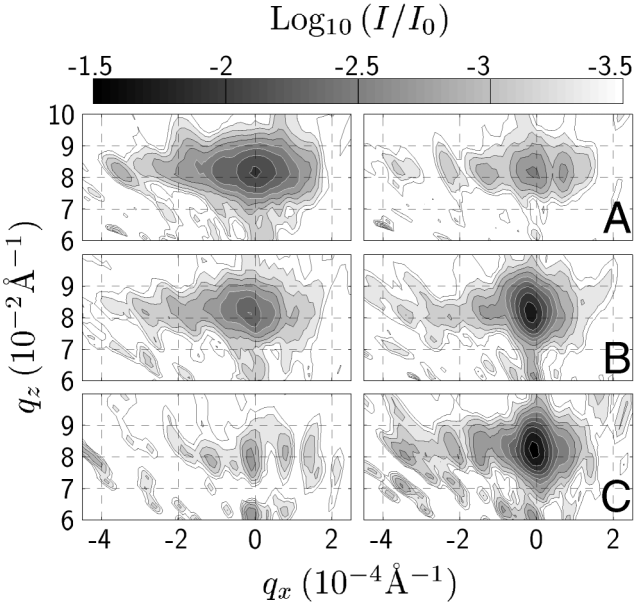

FIG. 2. Normalized neutron reflectivity maps. Polarized neutron intensity scattered specularly and off-specularly by a MgO(001)/[^{57}Fe(26 Å)/Cr(13 Å)]$_{20}$ ML in a magnetic field of (A) 7 mT, (B) 14.2 mT, and (C) 35 mT in R^{--} (left side) and in R^{-+} (right side) channels as a function of the scattering vector components q_x and q_z.

constants, the Fe saturation magnetization and measured values of the interlayer-coupling constant, and estimated values of the coercivity [24], the critical size of the patch domains in the PDS $\xi_c = 0.6-8.4$ μm was predicted [25], in accordance with the observed value of 2.6 μm. The domains are bound to their original sense of rotation as long as the magnetic field remains parallel to the [100] or to the $[\bar{1}00]$ direction, since the domain orientation is stabilized by the Zeeman energy in high fields and by the magnetocrystalline anisotropy energy in low fields.

The mechanism of BSF-induced *coarsening* basically differs from that of the PDS formation. Indeed, when an increasing magnetic field is applied in the *magnetization-parallel* ([010] or $[0\bar{1}0]$) direction, the anisotropy energy preserves the primary domain structure only for $H < H_{SF}$. At $H = H_{SF}$, the system becomes energetically unstable and the layer magnetizations flip to either the [100] or $[\bar{1}00]$ direction. There is again a freedom in the sense of rotation and, similar to H_S, also H_{SF} obeys a distribution. However, at $H \approx H_{SF}$ the system is close to an energy maximum and behaves like an explosive material: it may jump to an energy minimum by 90° or −90° rotation of the magnetization. Once the first region with the lowest value of H_{SF} "decides" between a 90° or −90° flop, it will "ignite" the neighbor regions, which will choose the same direction of magnetization to avoid creating new domain walls. In contrast to primary domain formation, secondary domains on BSF may grow *without any long-range domain-wall motion,* and this growth is, therefore, not limited by coercivity. BSF-induced domain coarsening is an *explosionlike 90° flop of the magnetization annihilating primary 180° walls* (and also the temporary 90° walls created during the BSF). Consequently, the secondary patch domain size may become comparable with the sample size.

The details of the PDS → SDS transition and the morphology of the resulting SDS depend on the correlation length ξ_{SF} of H_{SF} and also on how the domain-wall density scales with ξ. During the BSF, new nucleation centers may be formed beyond ξ_{SF}. If the "explosion" of a new center is fast enough so that the flopped domain becomes larger than ξ_c before it will be surrounded by a domain of opposite layer magnetization, it survives as an inclusion; otherwise it disappears. In fact, such inclusions are stable only for $\xi > \xi_c$ [25]. This qualitatively explains the observed coexistence of small and large domains in the SDS but a detailed model calculation is not yet available.

In conclusion, off-specular SMR and PNR evidenced a field-history dependent AF domain structure in a coupled Fe/Cr superlattice. Leaving the saturation region, a primary small-domain state is created in remanence. From this, when the system passes a BSF transition, a secondary domain state is formed that predominantly consists of large domains. The presented model gives a new insight into the nature of the domain transformation (with obvious implications on the transport noise) and lifts the controversy in the literature by showing that the condition for domain coarsening is not the equilibrium of the Zeeman energy with the domain-wall energy, but *the equilibrium of the Zeeman energy with the anisotropy energy.* It is only this equilibrium that permits the minute AF domain-wall energy to radically shape the domain structure. Out of this equilibrium the Zeeman energy and the anisotropy energy, whichever is greater, assist the coercivity in stabilizing the actual domain structure.

This work was partly supported by the Hungarian Scientific Research Fund (OTKA) under Contract No. T029409, the Flemish-Hungarian bilateral Project (20/98), and the European Communities (Contract No. ICA1-CT-2000-70029). The authors acknowledge helpful discussions with Dr. E. Kunnen, Dr. Yu. V. Nikitenko, and Dr. K. Temst. B. D. and J. M. thank the Belgian Science Foundation (F.W.O.-Vlaanderen) for financial support.

[1] P. Grünberg *et al.,* Phys. Rev. Lett. **57**, 2442 (1986).
[2] S. S. P. Parkin, N. More, and K. P. Roche, Phys. Rev. Lett. **64**, 2304 (1990).
[3] J. Unguris, R. J. Celotta, and D. T. Pierce, Phys. Rev. Lett. **67**, 140 (1991).
[4] M. N. Baibich *et al.,* Phys. Rev. Lett. **61**, 2472 (1988).
[5] H. T. Hardner, M. B. Weissmann, and S. S. P. Parkin, Appl. Phys. Lett. **67**, 1938 (1995).
[6] M. Rührig *et al.,* Phys. Status Solidi A **125**, 635 (1991).
[7] R. Schäfer, J. Magn. Magn. Mater. **148**, 226 (1995).
[8] N. Persat, H. A. M. van den Berg, and K. Cherifi-Khodjaoui, J. Appl. Phys. **81**, 4748 (1997).
[9] S. Langridge *et al.,* Phys. Rev. Lett. **85**, 4964 (2000).
[10] G. P. Felcher, Physica (Amsterdam) **192B**, 137 (1993).
[11] V. Lauter-Pasyuk *et al.,* Physica (Amsterdam) **283B**, 194 (2000).
[12] T. P. A. Hase *et al.,* Phys. Rev. B **61**, R3792 (2000).
[13] Unless otherwise stated, all domain properties (size, orientation, etc.) will be meant for the remanent state.
[14] N. Persat *et al.,* J. Magn. Magn. Mater. **165**, 446 (1997).
[15] L. J. Heyderman, J. N. Chapman, and S. S. P. Parkin, J. Appl. Phys. **76**, 6613 (1994).
[16] D. L. Nagy *et al.,* Hyperfine Interact. **126**, 353 (2000).
[17] R. Rüffer and A. I. Chumakov, Hyperfine Interact. **97/98**, 589 (1996).
[18] L. Bottyán *et al.,* J. Magn. Magn. Mater. **240**, 514 (2002).
[19] L. Bottyán *et al.,* in *ESRF Highlights 1999* (European Synchrotron Radiation Facility, Grenoble, 2000), p. 62, available through http://www.esrf.fr/.
[20] http://nfdfn.jinr.ru/fks/spn.html
[21] K. Temst *et al.,* Physica (Amsterdam) **276B–278B**, 684 (2000).
[22] R. W. Wang *et al.,* Phys. Rev. Lett. **72**, 920 (1994).
[23] R. W. Wang and D. L. Mills, Phys. Rev. B **50**, 3931 (1994).
[24] The coercivity of a fully compensated AF-coupled ML cannot be measured directly. Therefore, data measured on similar ferromagnetically coupled samples were used.
[25] D. L. Nagy *et al.,* Phys. Status Solidi A **189**, 591 (2002).